

## Facile Construction of pH- and Redox-Responsive Micelles from a Biodegradable Poly( $\beta$ -hydroxyl amine) for Drug Delivery

Dawei Li, Yazhong Bu, Lining Zhang, Xing Wang, Yanyu Yang, Yaping Zhuang, Fei Yang, Hong Shen, and De-Cheng Wu

*Biomacromolecules*, **Just Accepted Manuscript** • DOI: 10.1021/acs.biomac.5b01394 • Publication Date (Web): 18 Dec 2015

Downloaded from <http://pubs.acs.org> on December 22, 2015

### Just Accepted

“Just Accepted” manuscripts have been peer-reviewed and accepted for publication. They are posted online prior to technical editing, formatting for publication and author proofing. The American Chemical Society provides “Just Accepted” as a free service to the research community to expedite the dissemination of scientific material as soon as possible after acceptance. “Just Accepted” manuscripts appear in full in PDF format accompanied by an HTML abstract. “Just Accepted” manuscripts have been fully peer reviewed, but should not be considered the official version of record. They are accessible to all readers and citable by the Digital Object Identifier (DOI®). “Just Accepted” is an optional service offered to authors. Therefore, the “Just Accepted” Web site may not include all articles that will be published in the journal. After a manuscript is technically edited and formatted, it will be removed from the “Just Accepted” Web site and published as an ASAP article. Note that technical editing may introduce minor changes to the manuscript text and/or graphics which could affect content, and all legal disclaimers and ethical guidelines that apply to the journal pertain. ACS cannot be held responsible for errors or consequences arising from the use of information contained in these “Just Accepted” manuscripts.



# Facile Construction of pH- and Redox-Responsive Micelles from a Biodegradable Poly( $\beta$ -hydroxyl amine) for Drug Delivery

Dawei Li,<sup>†,‡,§</sup> Yazhong Bu,<sup>†,§</sup> Lining Zhang,<sup>§</sup> Xing Wang,<sup>\*,†</sup> Yanyu Yang,<sup>†</sup> Yaping Zhuang,<sup>†</sup> Fei Yang,<sup>†</sup> Hong Shen<sup>†</sup> and Decheng Wu<sup>\*,†</sup>

<sup>†</sup>Beijing National Laboratory for Molecular Sciences, State Key Laboratory of Polymer Physics & Chemistry, Institute of Chemistry, Chinese Academy of Sciences, Beijing 100190, China

<sup>‡</sup>Department of Orthopaedics, The 309<sup>th</sup> Hospital of the PLA, Beijing 100094, China

<sup>§</sup>Center of Rehabilitation, Chinese People's Liberation Army General Hospital, Fuxing Road, Beijing, 100853, China

KEYWORDS: disulfide, cationic polymer, micelles, dual-responsive, drug delivery.

**ABSTRACT:** Here we demonstrate a type of pH and reduction dual-sensitive biodegradable micelles, which were self-assembled by a cationic polymer in an aqueous solution. Due to tumor cells or tissues showing low pH and high reduction concentration, these micelles possessed specific tumor targetability and maximal drug-release controllability inside tumor cells upon changes in physical and chemical environments, but presented good stability at physiological

1  
2  
3 conditions. CCK-8 assay showed that the DOX-loaded micelles had a similar cytotoxicity for  
4 MCF-7 tumor cells as free DOX, and blank micelles had a very low cytotoxicity to the cells.  
5  
6  
7  
8  
9  
10  
11  
12  
13  
14  
15  
16  
17  
18  
19  
20  
21  
22  
23  
24  
25  
26  
27  
28  
29  
30  
31  
32  
33  
34  
35  
36  
37  
38  
39  
40  
41  
42  
43  
44  
45  
46  
47  
48  
49  
50  
51  
52  
53  
54  
55  
56  
57  
58  
59  
60

Fluorescent microscopy observation revealed that the drug-loaded micelles could be quickly internalized by endosomes to inhibit cancer cell growth. These results indicated these biodegradable micelles, as a novel and effective pH- and redox-responsive nanocarrier, have a potential to improve drug delivery and enhance the antitumor efficacy.

## INTRODUCTION

Biodegradable polymeric micelles in aqueous solutions have been extensively explored as a most promising candidate in drug delivery systems for targeted cancer chemotherapy.<sup>1-4</sup> To overcome severe problems that are associated with traditional hydrophobic antitumor drugs, polymeric micellar nanocarriers need to possess several unique advantages, including good water solubility, long *in vivo* circulation times, efficient bioavailability, high preferential accumulation at the tumor sites and low systemic side effects.<sup>5</sup> Specially, stimuli-responsive micelles were furnished for specific tumor targetability and maximal drug release controllability inside the target cells upon changes in physical and chemical environments, such as redox, pH, temperature, magnetism, ultrasound, enzyme and glucose.<sup>6</sup>

The significantly chemical stimuli to trigger drug release were pH and redox. In general, pH maintains about 7.4 in normal extracellular matrices and blood while tumors always presented a weak acid in the intracellular compartments due to low oxygen in intercellular environments.<sup>7</sup> When drug carriers were endocytosed into endosomes, the carriers firstly encountered a pH with 5.5-6.5 in the early endosomes, then pH declined into about 5.0 in the later endosomes, and

1  
2  
3 finally lysosomes decrease even lower pH value. Accordingly, pH-responsive polymeric micelles  
4 have been widely developed for targeted tumor or tissue in biological systems. As one of  
5  
6 representative instances, tertiary amine group was generally introduced into polymers to control  
7  
8 assembled behaviors by protonation/deprotonation.<sup>8</sup>  
9  
10

11  
12  
13  
14 Redox-responsive micelles have own unique potential to facilitate drug release in tumor cells  
15  
16 or tissues, which is originated from varied concentrations of redox species in intracellular and  
17  
18 extracellular compartments.<sup>9</sup> For example, glutathione (GSH) is a most abundant reductive  
19  
20 molecule with millimolar concentrations in the intracellular compartments (~10 mM in the  
21  
22 cytoplasm) and micromolar concentrations in the extracellular environment (~10  $\mu$ M in the  
23  
24 plasma). The disulfide bond is stable under physiological conditions during circulation as well as  
25  
26 in the extracellular tissues on account of a low concentration of GSH, but quickly cleaved upon  
27  
28 exposure to a highly reductive environment in cells.<sup>10</sup> Therefore, utilizing disulfide-containing  
29  
30 redox-responsive micelles for drug carrier has been a biologically and friendly method for drug  
31  
32 delivery.  
33  
34  
35

36  
37  
38 Cationization of polymers is another approach that can be applied for targeted drug  
39  
40 delivery.<sup>11,12</sup> The cell surface membrane is negatively charged, so this charged surface provides  
41  
42 plentiful sites of interaction for cationic macromolecules. Therefore, cationic delivery systems  
43  
44 have been utilized for the delivery of drugs, proteins and genes to various tissues including liver,  
45  
46 brain and kidney.<sup>13</sup> In recent years, amine–epoxy “click” reaction between di-amine and di-  
47  
48 epoxy groups has been recognized as a facile access to prepare main-chain cationic polymers.<sup>14</sup>  
49  
50 This method offers many natural advantages: 1) the polymerization proceeds at room  
51  
52 temperature without any catalyst; 2) the coupling reaction produces equivalent reactive hydroxyl  
53  
54 groups that are convenient for further functionalization; 3) many tertiary amines are generated  
55  
56  
57  
58  
59  
60

1  
2  
3 upon the polymerization that can be transformed into positively charge quaternary structures by  
4 protonation/alkylation. Therefore, a reactive polymer scaffold with several chemically distinct  
5 functional sites can be created at ambient conditions in one simple step by amine–epoxy  
6 reaction. This family of main-chain cationic polymers is named as poly( $\beta$ -hydroxyl amine)s  
7 (PHA), which has a weakly basic characteristic on account of its tertiary amines with a pK<sub>b</sub>  
8 value of about 6.5. Self-assembly of the biodegradable poly( $\beta$ -hydroxyl amine)s has been studied  
9 in recent years, but due to poor hydrophilicity provided by hydroxyl groups and tertiary amines,  
10 the main-chain cationic polymers always were linked by hydrophilic segments or polymers to  
11 build amphiphilic copolymers and corresponding stimuli-responsive copolymeric micelles in  
12 water for intracellular doxorubicin delivery.<sup>15</sup>  
13  
14  
15  
16  
17  
18  
19  
20  
21  
22  
23  
24  
25  
26  
27

28 Here, we reported a facile method to construct pH- and redox-responsive micelles from a  
29 novel reducible poly( $\beta$ -hydroxyl amine)s (RPHA), in which a large number of hydroxyl groups  
30 gave rise to good hydrophilicity to stable micelles in aqueous solutions, and the abundant  
31 disulfide bonds embedded in the core and tertiary amines located in the shell provided the  
32 stimulative responsibility for the micelles. The RPHA polymer and its micelles possessed many  
33 unique advantages: 1) the RPHA polymer was easily prepared at ambient conditions in one  
34 simple step by amine–epoxy “click” reaction; 2) a large number of disulfides in the inner  
35 micelles maintain the compact core-shell architectures in the normal physiological conditions,  
36 but are high sensitive to reductive agents in a short time, which can facilitate intracellular rapid  
37 release of the encapsulated drugs within the cells; 3) abundant tertiary amines endow the PRHA  
38 polymer high buffer capacity in a certain pH range; 4) massive hydroxyl groups allow  
39 convenient post-functionalization to yield multifunctional aggregations; 5) these particles would  
40 be demicellized rapidly into water-soluble molecules at high levels of reducing agents and/or in  
41  
42  
43  
44  
45  
46  
47  
48  
49  
50  
51  
52  
53  
54  
55  
56  
57  
58  
59  
60

1  
2  
3 an acidic environment, which was benefit for antitumor drug to release from the carriers when  
4  
5 the pH values and concentrations of reducing agents changed in intracellular and extracellular  
6  
7 compartments. Additionally, a few of hydroxyl groups were further modified by coumarins to  
8  
9 yield the RPHA-g-coumarin polymer, and its corresponding spherical micelle exhibited high  
10  
11 fluorescence intensity in aqueous solutions.  
12  
13

## 14 15 16 **EXPERIMENTAL SECTION**

17  
18  
19 **Materials.** Potassium tert-butanolate (99%, J&K), 2,2'-dithiodiethanol (90%, Energy Chemical),  
20  
21 epibromohydrin (97%, Energy Chemical), ethanolamine (99%, J&K), dithiothreitol (DTT, 99%,  
22  
23 J&K), 2-Hydroxybenzaldehyde (99%, J&K), diethyl malonate (99.5%, J&K), diethylamine (99%,  
24  
25 J&K), 4-(dimethyl-amino)-pyridine (DMAP, 99%, Aldrich), triethylamine (TEA, 99%, Beijing  
26  
27 Chemical Works), thionyl chloride (SOCl<sub>2</sub>, 99.5%, Energy Chemical), sodium hydroxide,  
28  
29 ethanol, acetic acid glacial, ethyl acetate, hydrochloric acid, acetone, isopropanol, hexane and  
30  
31 ether (reagent grade, Beijing Chemical Works), tetrahydrofuran (THF), *N,N*-dimethyl formamide  
32  
33 (DMF), chloroform (CHCl<sub>3</sub>) and dichloromethane (CH<sub>2</sub>Cl<sub>2</sub>) were purified by stirring over  
34  
35 calcium hydride for 24 h followed by distillation.  
36  
37  
38  
39  
40

41  
42 **Characterizations.** <sup>1</sup>H and <sup>13</sup>C NMR spectra were obtained on a Bruker DRX-400 spectrometer.  
43  
44 Gel permeation chromatography (GPC) measurement was carried out on a system comprised of a  
45  
46 Waters 515 HPLC pump, and a Waters 2414 RI detector equipped with four Waters Styragel  
47  
48 columns (HT 2, HT 3, HT 4, and HT 5). DMF with 0.01 M LiBr was used as the eluent at a flow  
49  
50 rate of 1.0 mL/min. Polystyrene standards were used for the calibration. Transmission electron  
51  
52 microscopy (TEM) images were obtained on a JEM-2200FS microscope (JEOL, Japan). A 5 μL  
53  
54 droplet of micellar solution was dropped onto a copper grid (300 mesh) coated with a carbon film,  
55  
56  
57  
58  
59  
60

1  
2  
3 followed by drying at room temperature. The samples were sputter-coated with a thin layer of Pt  
4  
5 for 120 s to make the samples conductive before testing. Dynamic light scattering (DLS) spectra  
6  
7 were obtained on a commercial laser light scattering spectrometer (ALV/DLS/SLS-5022F)  
8  
9 equipped with a multi- $\tau$  digital time correlator (ALV5000) and a cylindrical 22 mW UNIPHASE  
10  
11 He-Ne laser ( $\lambda_0=632.8$  nm) was used. All data were averaged over three time measurements. The  
12  
13 laser light scattering cell is held in a thermostat index matching vat filled with purified and dust-  
14  
15 free toluene with the temperature controlled to within 0.1 °C. UV-vis spectra of the samples were  
16  
17 measured on a Hitachi U-3010 spectrometer, and fluorescence measurements were carried out on  
18  
19 a Hitachi F4600 photoluminescence spectrometer with a xenon lamp as a light source. Confocal  
20  
21 laser scanning microscopy (CLSM, Zeiss LSM 510, Germany) was under excitation at 314 nm.  
22  
23  
24  
25  
26  
27

28 **Synthesis of 2,2'-Dithiodiethanol Diepoxypropyl Ether.** In a 250 mL round-bottomed flask  
29  
30 equipped with a magnetic stirring bar, potassium tert-butanolate (4.48 g, 40 mmol) and 2,2'-  
31  
32 dithiodiethanol (3.08 g, 20 mmol) were dissolved in 50 mL of isopropanol, followed by addition  
33  
34 100 mL of isopropanol containing epibromohydrin (6.85 g, 50 mmol) to fully dissolve all the  
35  
36 solids. The reaction was allowed to proceed for 24 h at room temperature. After that, the mixture  
37  
38 was filtrated and the crude product was yielded after removing the solvent. Then the final  
39  
40 product was separated chromatographically on silica gel with ethyl acetate/hexane (v/v=2/1) to  
41  
42 afford the yellow viscous liquid with 33.5% yield.  
43  
44  
45  
46  
47

48 **Synthesis of Coumarin-3-carboxylic Acid.** In a 100 mL round-bottomed flask equipped with a  
49  
50 magnetic stirring bar, 2-hydroxybenzaldehyde (12.2 g, 0.1 mol), diethyl malonate (19.2 g, 0.12  
51  
52 mol), diethylamine (1.8 g, 0.025 mol) and acetic acid glacial (1 mL) were dissolved in 30 mL of  
53  
54 ethanol. After refluxing for 2 h, a mount of NaOH solution was added into the mixture, and then  
55  
56 kept refluxing for another 15 min. After cooling to the room temperature, a mount of  
57  
58  
59  
60

1  
2  
3 concentrated hydrochloric acid was added to adjust pH = 2 to produce the solid precipitates in an  
4  
5 ice bath. The crude products were obtained after filtration, washing with DI water and drying.  
6  
7  
8 Then recrystallization from ethanol afforded the white solid with 77.2% yield.  
9

10  
11 **Synthesis of Coumarin-3-acyl Chloride.** Coumarin-3-carboxylic acid (1.9 g, 10 mmol) and two  
12  
13 drops of DMF were added into 6 mL of SOCl<sub>2</sub>. The mixture was stirred at room temperature for  
14  
15  
16  
17 2 h and concentrated under reduced pressure to afford the faint yellow solid with 87.8% yield.  
18  
19

20  
21 **Synthesis of Reducible Poly( $\beta$ -hydroxy amine)s (RPHA) Polymer.** 2,2'-dithiodiethanol  
22  
23 diepoxypropyl ether (267 mg, 1 mmol) and ethanolamine (61 mg, 1 mmol) were dissolved in 5  
24  
25 mL of methanol. After stirring for several days at room temperature, the mixture was precipitated  
26  
27 in a large excess amount of diethyl ether twice and dried in vacuum to afford the final product  
28  
29 with 85.4% yield.  
30  
31

32  
33 **Synthesis of RPHA-g-coumarin Polymer.** RPHA (240 mg, 0.02 mmol) and DMAP (5 mg, 0.04  
34  
35 mmol) were dissolved in 5 mL of anhydrous DMF. Under vigorous stirring at 0 °C, coumarin-3-  
36  
37 acry chloride (34 mg, 0.16 mmol) was dropwise into the solution for 30 min. The solution was  
38  
39 stirred at room temperature for another 4 h, and precipitated in ether for three times to afford the  
40  
41 white solid with 84.7% yield.  
42  
43  
44  
45

46  
47 **Formation and Self-assembly of the Amphiphilic RPHA Polymer.** Polymeric micelles were  
48  
49 prepared by a dialysis method. A typical self-assembly aggregate solution was prepared as  
50  
51 following: RPHA polymer (5 mg) was first dissolved in methanol (1 mL). Then deionized water  
52  
53 (4 mL) was added dropwise into the solution at the rate of 0.05 mL/min via a syringe pump. The  
54  
55 colloidal dispersion was further stirred for another 2 h and the temperature was fixed at 30 °C  
56  
57  
58  
59  
60

1  
2  
3 during the self-assembling process. The organic solvent was removed by dialysis (MW cutoff, 4  
4 kDa) against deionized water for 3 days.  
5  
6

7  
8  
9 **Determination of pH and Reduction-Triggered Destabilization of RPHA Micelles.** The size  
10 change of micelles in response to DTT in phosphate buffered saline (PBS, pH 7.4) or PBS (pH  
11 5.0) was determined by DLS measurement. For determining the reduction sensitivity of micelles,  
12 DTT (10 mM) was added into a 10 mL solution of RPHA micelles (1 mg/mL) in PBS (pH 7.4),  
13 and then the solution was mildly stirring at 37 °C. After 8 h, the size was measured by DLS. For  
14 determining the pH sensitivity of micelles, a certain amount of PBS (pH 5.0) was added into 10  
15 mL solution of RPHA micelles (1 mg/mL), and then the solution was mildly stirring at 37 °C.  
16 After 8 h, the size was measured by DLS.  
17  
18  
19  
20  
21  
22  
23  
24  
25  
26  
27

28  
29 **Formation and Self-assembly of RPHA-g-coumarin Polymer.** Polymeric micelles were  
30 prepared by a dialysis method. A typical self-assembly aggregate solution was prepared as  
31 following: RPHA polymer (5 mg) was first dissolved in methanol (1 mL), and then deionized  
32 water (4 mL) was added dropwise into the solution at the rate of 0.05 mL/min via a syringe  
33 pump. The colloidal dispersion was further stirred for another 2 h and the temperature was fixed  
34 at 30 °C during the self-assembling process. The organic solvent was removed by dialysis (MW  
35 cutoff, 4 kDa) against deionized water for 3 days.  
36  
37  
38  
39  
40  
41  
42  
43  
44  
45

46 **Preparation of DOX-Loaded RPHA Micelles.** DOX-loaded micelles were prepared as follows:  
47 20 mg RPHA was dissolved in 1 mL of DMF, followed by adding a predetermined amount of  
48 DOX·HCl and 1.5 molar equiv of triethylamine and stirred at room temperature for 2 h. Then 4  
49 mL of phosphate buffered saline (PBS, pH 7.4) was added dropwise into the solution at the rate  
50  
51  
52  
53  
54  
55  
56  
57  
58  
59  
60

1  
2  
3 of 0.05 mL/min via a syringe pump. Subsequently, the solution was dialyzed against deionized  
4  
5 water for 24 h (MW cutoff, 4 kDa) to remove free DOX and byproducts.  
6  
7

8  
9 ***In Vitro* DOX Release from Polymeric Micelles.** The pH-dependent DOX release  
10  
11 measurements were conducted as below: dispersed DOX-loaded polymeric micelles were added  
12  
13 into a dialysis membrane tube (MW cutoff, 4 kDa), which was then incubated in 30 mL of  
14  
15 phosphate buffer saline (PBS) at pH 5.0 or 7.4 at 37 °C in a shaking water bath at rate of 90 rpm.  
16  
17 The DTT-dependent DOX release measurements were conducted in the same manner as  
18  
19 described above. The incubation solutions were 30 mL of PBS (pH 7.4) with DTT concentrations  
20  
21 of 10 mM. At predetermined frequencies, 6 mL of incubated solution was taken out and 6 mL of  
22  
23 fresh PBS with 10 mM of DTT was added to refill the incubation solution to 30 mL. The pH-  
24  
25 dependent DOX release profiles were determined by measuring the UV-vis absorbance of the  
26  
27 solutions at 480 nm. All DOX-release experiments were conducted in triplicate and the results  
28  
29 were expressed as the average data with standard deviations. To determine the total loading of  
30  
31 the drug, the DOX-loaded micellar suspensions were freeze-dried and then dissolved in DMF  
32  
33 again, and analyzed with fluorescence spectroscopy. A calibration curve was obtained using  
34  
35 DOX/DMF solutions with different DOX concentrations. For determining the amount of DOX  
36  
37 release, calibration curves were running with DOX/phosphate buffer solution (pH 7.4, 100 mM)  
38  
39 with different DOX concentrations. Release experiments were conducted in triplicate. The  
40  
41 results were presented as the average  $\pm$  standard deviation.  
42  
43  
44  
45  
46  
47  
48

49  
50 Drug loading content (DLC) and drug loading efficiency (DLE) were calculated according to the  
51  
52 following formulas:  
53  
54

$$55 \\ 56 \text{DLC (wt \%)} = (\text{weight of loaded drug/weight of polymer}) \times 100\% \\ 57 \\ 58 \\ 59 \\ 60$$

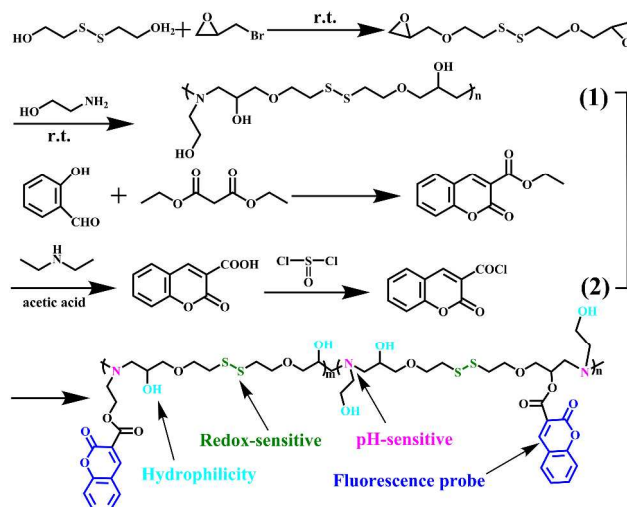
1  
2  
3 DLE (wt %) = (weight of loaded drug/weight of feeding drug)  $\times$  100%  
4  
5

6 **Fluorescent Microscope Observation of MCF-7 cells Incubated with DOX-Loaded**

7 **Polymeric Micelles.** MCF-7 cells were plated on microscope slides in a 96-well plate ( $5 \times 10^4$   
8 cells/well) using Dulbecco's Modified Eagle medium (DMEM) medium containing 10% FBS.  
9 After incubation for 24 h, the cells were incubated with prescribed amounts of DOX-loaded  
10 RPHA micelles or free DOX at 37 °C and 5% CO<sub>2</sub> for another 24 h. Then the culture medium  
11 was removed and the cells on microscope plates were washed three times with PBS. After fixing  
12 with 4% paraformaldehyde overnight, the cells were observed under a fluorescent microscope.  
13  
14  
15  
16  
17  
18  
19  
20  
21  
22  
23

24 **CCK-8 Assay.** The cytotoxicity of RPHA micelles and DOX-loaded RPHA micelles was  
25 studied by CCK-8 assay using MCF-7 cells. Cells were seeded onto a 96-well plate at a density  
26 of  $1 \times 10^4$  cells per well in 180  $\mu$ L of DMEM containing 10% fetal bovine serum (FBS) and  
27 incubated for 24 h (37 °C, 5% CO<sub>2</sub>). The medium was replaced by 90  $\mu$ L of fresh DMEM  
28 medium containing 10% FBS, and then 20  $\mu$ L samples of various concentrations (2-10 mg/mL)  
29 of the micelle suspensions in PBS (pH 7.4) were added. The cells were incubated for another 24  
30 h. After removal of the culture media from cell culture plates, 100  $\mu$ L fresh culture media and 10  
31  $\mu$ L CCK-8 kit solutions were immediately added and homogeneously mixed and then incubated  
32 for 4 h in a CO<sub>2</sub> incubator. Finally, 100  $\mu$ L reaction solutions were put into 96-well plate. The  
33 optical density of each well at 450 nm was read by a microplate reader. Cells cultured in DMEM  
34 medium containing 10% FBS (without exposure to micelles) were used as controls.  
35  
36  
37  
38  
39  
40  
41  
42  
43  
44  
45  
46  
47  
48  
49  
50  
51  
52  
53  
54  
55  
56  
57  
58  
59  
60

**Scheme 1.** Synthetic Route of pH- and Redox-Sensitive RPHA and RPHA-g-Coumarin Polymers

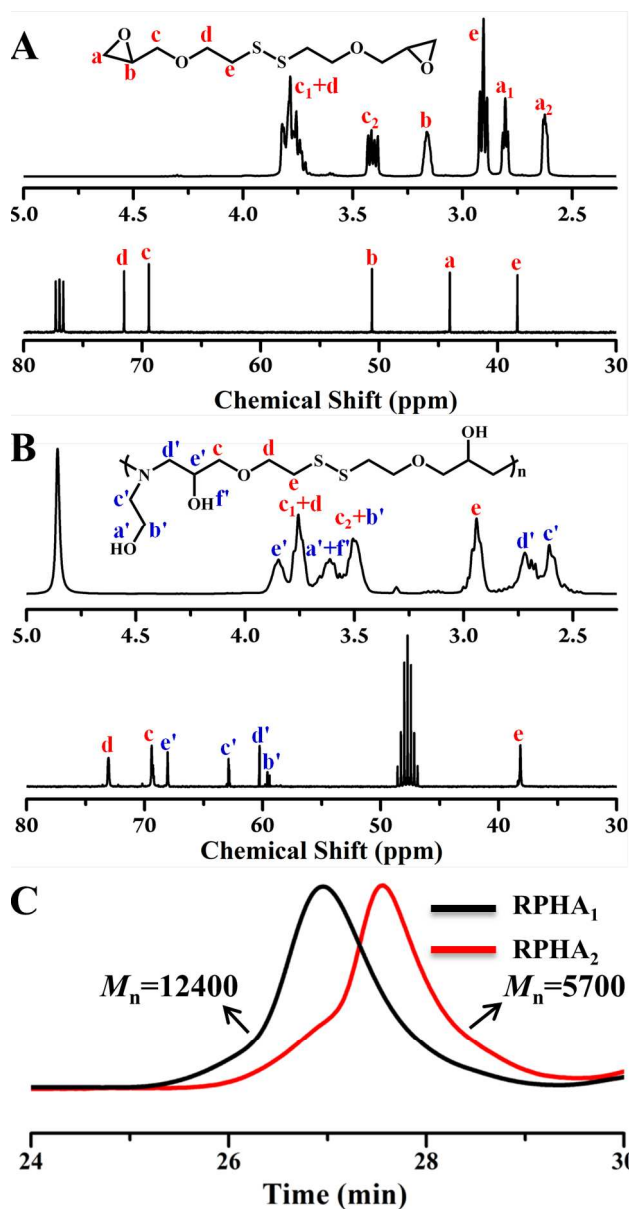


## RESULTS AND DISCUSSION

### Synthesis and Characterization of the Reducible Poly( $\beta$ -hydroxyl amine)s (RPHA).

Synthetic pathway of the RPHA polymer is summarized in Scheme 1. Firstly, the monomer of 2,2'-dithiodiethanol diepoxypropyl ether (Figure 1A) was produced with high purity, and then reacted with ethanolamine to yield cationic RPHA polymers by amine–epoxy reaction at room temperature. Two polymers, RPHA<sub>1</sub> and RPHA<sub>2</sub>, were produced after polymerization of 5 and 3 days. The every repetitive unit of this cationic polymer possessed a disulfide bond, a tertiary amine and three hydroxyl groups. Figure 1B showed the clear assignment of the polymeric framework. The typical epoxy proton resonances at 2.6, 2.8 and 3.1 ppm disappeared, and the expected shifts in the proton resonances, such as methylene groups and hydroxyl groups, appeared after polymerization in the <sup>1</sup>H NMR spectra (Figure 1A and 1B). The chemical structures of the monomer and RPHA polymer were further clearly clarified in the <sup>13</sup>C NMR spectra of the monomer (Figure 1A) and RPHA polymer (Figure 1B). Figure 1C gave the

molecule weights of two polymers were about 5700 and 12400, and the corresponding polydispersity indices were 1.83 and 2.23, respectively. It is mentioned that the monomer stoichiometry and the polymerization time are two critical factors to define  $M_n$  of RPHA polymers in the step-growth polymerization. These results manifested a simple synthetic pathway for preparation of reducible poly( $\beta$ -hydroxyl amine)s in a mild condition.



1  
2  
3 **Figure 1.**  $^1\text{H}$  and  $^{13}\text{C}$  NMR spectra of (A) monomer and (B) RPHA<sub>1</sub>. (C) GPC curves of the  
4  
5 RPHA polymers.  
6  
7

8  
9 **Formation and pH- and Redox-Triggered Disruption of Micelles.** Due to a large number of  
10 hydrophilic hydroxyl groups and tertiary amines throughout the polymer backbone, these main-  
11 chain cationic RPHA polymers were recognized as a novel amphiphilic polymer that can be self-  
12 assembled into nanometre aggregations in aqueous solutions. We investigated self-assembly  
13 behaviours of the two polymers. The RPHA<sub>1</sub> polymer could assemble into the stable micelles,  
14 but the assemblies of the RPHA<sub>2</sub> polymer quickly precipitated after dialysis with water. The poor  
15 stability of the RPHA<sub>2</sub>-based assemblies in water may ascribe to that the hydrophobic terminal  
16 epoxy groups have a certain effect on hydrophobicity /hydrophilicity balance when the repeat  
17 units are not so high. So we adopted the RPHA<sub>1</sub> polymer to systemically explore its self-  
18 assembly and drug-release behaviours. The CMC of RPHA micelles was ca. 1.17 mg/L as  
19 determined by fluorescence measurements using pyrene as a probe. Transmission electron  
20 microscope (TEM) images in Figure 2A showed formation of the uniform spherical micelles, and  
21 the average diameter is about 85 nm. Dynamic light scattering (DLS) revealed a large  
22 hydrodynamic diameter of 185 nm and a PDI of 0.29 in Figure 2D. The bigger size was  
23 attributed to the swollen molecules in water, indicating high hydrophilicity given by excess  
24 pendant hydroxyl groups. This size of RPHA<sub>1</sub> micelles is suitable for intracellular drug delivery,  
25 because an appropriate diameter (less than 200 nm) of aggregations is favourable to keep the  
26 lowered level of reticuloendothelial system (RES) uptake, minimal renal excretion and efficient  
27 EPR effect for passive tumour-targeting.<sup>16</sup>  
28  
29  
30  
31  
32  
33  
34  
35  
36  
37  
38  
39  
40  
41  
42  
43  
44  
45  
46  
47  
48  
49  
50  
51  
52  
53  
54  
55  
56  
57  
58  
59  
60

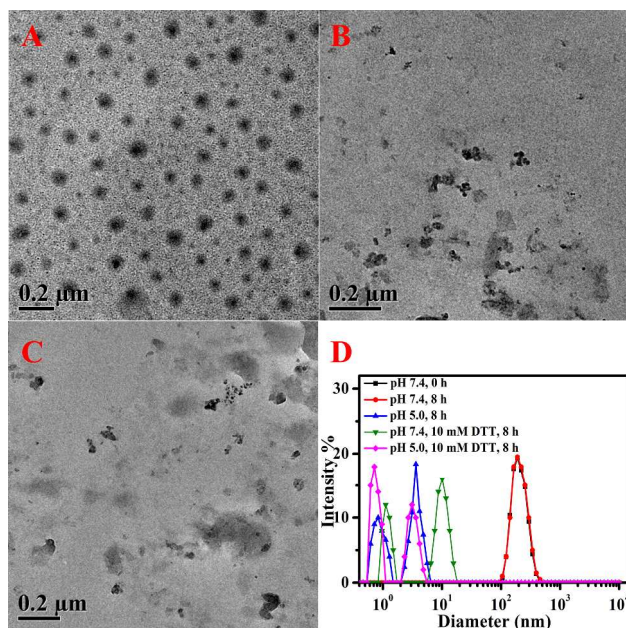


**Figure 2.** TEM images of the micelles before (A) and after treatment of (B) pH 5.0 and (C) 10 mM DTT for 8 h. (D) The size change of the micelles in response to 10 mM DTT in PBS (pH 7.4 or 5.0) and at 37 °C for 8 h determined by DLS measurement (micelles without any treatments were used as the control).

A lot of disulfide bridge linkages, served as the hydrophobic moieties of micelles, were throughout the whole polymeric main chain. Accordingly, the RPHA micelles can inevitably be broken down in response to the reductive agents. Meanwhile, the same number of tertiary amines in the architectural framework furnished the micelles breakable behaviour with pH-responsive property, because tertiary amines can be protonated to give cationic backbones that can be dissolved in water. Therefore, these micelles possessed pH and reduction dual-responsive properties. To study this pH- and redox-triggered disassembly responsiveness, the micelles were treated with 10 mM DTT and/or in acidic conditions. The particle size changes of the micelles were measured by DLS measurement. After adjusting pH value of the solution to 5.0, the micelles were damaged as observed in Figure 2B corresponding to the diameters of about 0.3 and

7 nm (Figure 2D). Similarly, for the reducible moiety, polymeric micelles were degraded in the presence of a high level of DTT (10 mM) that triggered the disassembly of micelles in Figure 2C. The corresponding sizes of DLS profile were ca. 1 and 10 nm in Figure 2D, demonstrating DTT-triggered cleavage of disulfide bonds and dissociation of the aggregation. As a control, the size of micelles had no obvious alteration after 8 h immersion in PBS buffer (pH=7.4) without DTT.

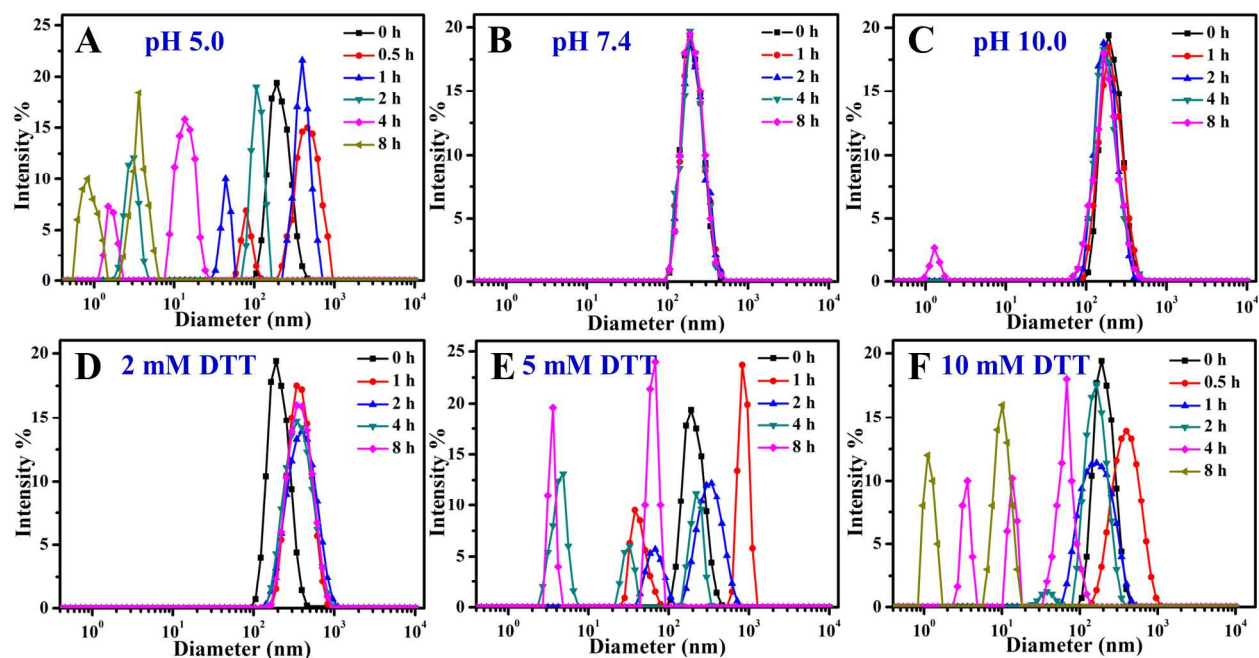


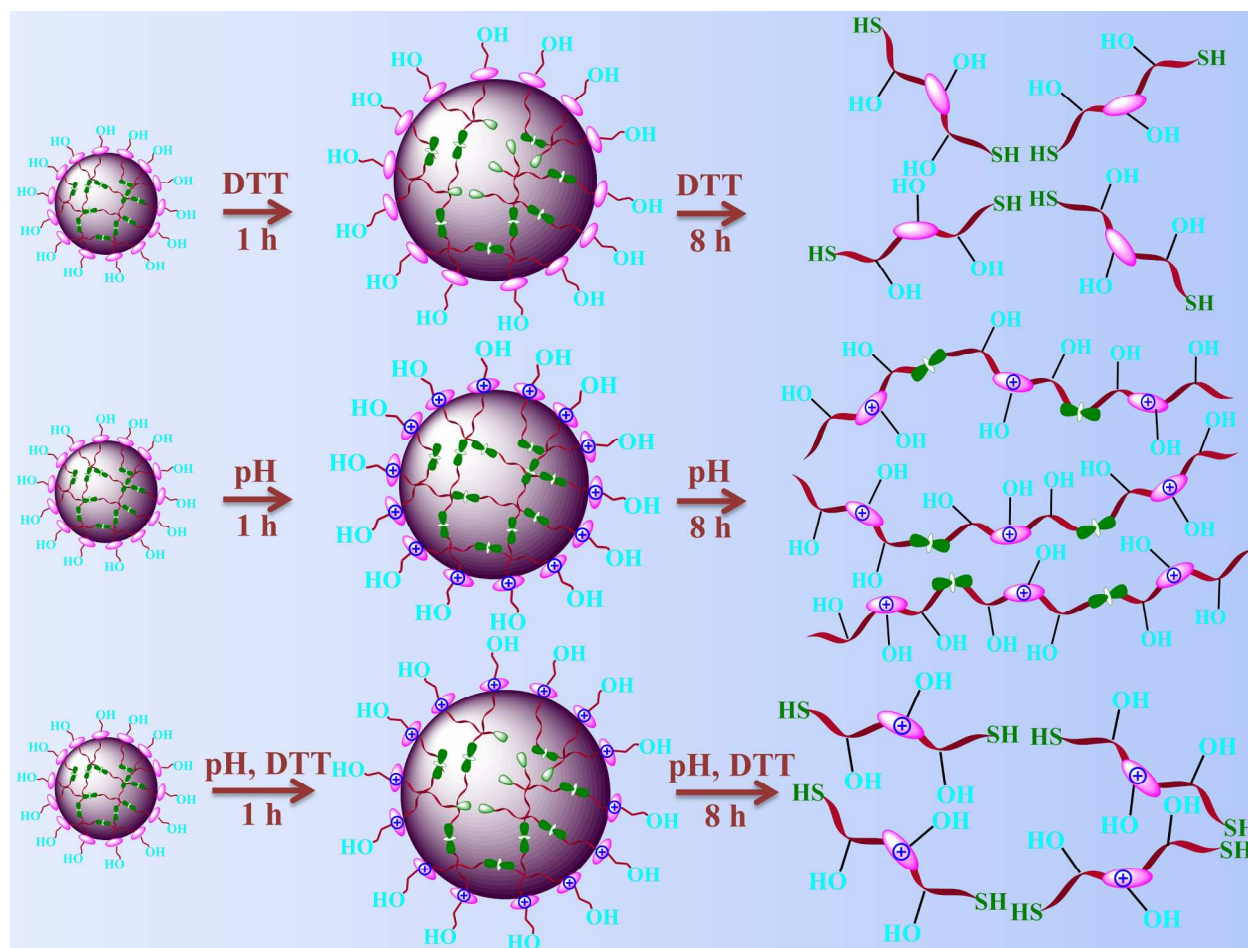
**Figure 3.** The size change of the micelles in response to (A) pH 5.0, (B) pH 7.4, (C) pH 10.0, (D) 2 mM, (E) 5 mM and (F) 10 mM DTT in PBS (pH 7.4) at 37 °C for various treated time determined by DLS measurement.

We further quantitated the different pH (5.0, 7.4 and 10.0) and DTT concentration (2 mM, 5 mM and 10 mM) conditions at various treated time to study the biodegradation process of particles by DLS measurement. By adjusting pH value of the solution to 5.0 for 0.5 h shown in Figure 3A, the swelling and cracking of the polymeric micelles could be observed corresponding to one peak with up to 450 nm and another peak with 80 nm. Then the size declined into 393 nm

1  
2  
3 and 45 nm after 1 h. The incremental size ascribed to electrostatic repulsive force and the  
4 micellar swelling originated from the protonated tertiary amines and improved hydrophilicity.  
5  
6 The shrunken size resulted from the partially destroyed micelles. After treatment for 2 h,  
7  
8 protonated tertiary amines markedly improved the solubility of RPHA polymers and the micelles  
9  
10 degraded into small particles, including the collapsed micelles and escaped polymeric chains  
11  
12 from the aggregates. With standing for the longer time, more and more polymeric chains were  
13  
14 released from the micelles. After 8 h, all the micelles decomposed into the protonated polymer  
15  
16 chains with the size of ca. 1-5 nm by DLS measurement. The nanoscale was in accordance with  
17  
18 the theoretic size ( $2.3 \pm 0.2$  nm) calculated by molecular dynamics (MD) simulation, proving  
19  
20 completely dissolution of micelles in pH 5.0 solution. In comparison, the micelles in pH 7.4 or  
21  
22 pH 10.0 can basically maintained the initial diameters (Figure 3B and 3C). As for DTT-triggered  
23  
24 disassembly of the micelles, some disulfides were broken down in the first 1 h in the presence of  
25  
26 2 mM DTT (Figure 3D), and thus the micelles became slightly loose and swollen with the size  
27  
28 increasing into 355 nm. However, the majority of intact disulfides preserved the micellar  
29  
30 architectures even after 8 h, indicating that a low concentration of DTT can hardly destroy the  
31  
32 micelle completely. When the DTT concentration increased up to 5 and 10 mM, the disulfide  
33  
34 linkages were easily broken down, inducing the micelles rapidly disassembled in the first 2 h  
35  
36 (Figure 3E and 3F). After 8 h, the disulfide linkages were completely cleaved to degrade the  
37  
38 micelles into small water-soluble molecules with the diameter of ca. 1-10 nm. It is mentioned  
39  
40 that high level of DTT concentration and acidic condition can work in tandem to accelerate the  
41  
42 degradation of micelles into water-soluble protonated molecules with smaller diameters of ca.  
43  
44 0.3-7 nm (Figure 2D), which was consistent with the MD simulation result ( $1.1 \pm 0.1$  nm). The  
45  
46 degradation processes by pH-triggered, DTT-triggered and pH-/DTT-triggered disassembly of  
47  
48  
49  
50  
51  
52  
53  
54  
55  
56  
57  
58  
59  
60

micelles were clearly illustrated in Scheme 2. These results further revealed these dual-sensitive micelles were stable in the normal physiological conditions and degradable in response to high concentration of reductive agents and/or acidic environment, which can be employed as an intelligent responsive drug carrier.

**Scheme 2.** Schematic of pH and/or DTT-Triggered the Demicellization of RPHA Micelles



**Loading and *In Vitro* Release of DOX.** DOX was loaded into the micelles by dialysis method.

The dialysate was analysed by fluorescence spectrum and the results showed the characteristic absorbance at 554 nm for DOX was not detected, demonstrating the free DOX was removed completely. The drug loading content in the micelles was 9.1%, and the corresponding drug

1  
2  
3 loading efficiency was 36.6%. The *in vitro* release of DOX from the micelles was firstly  
4 investigated at 37 °C under different conditions, i.e., (a) pH 7.4 in PBS, (b) pH 5.0 in PBS, (c) 10  
5 mM DTT and pH 7.4 in PBS, and (d) 10 mM DTT and pH 5.0 in PBS. As shown in Figure 4A, a  
6 slow release of below 20% of incorporated DOX within 24 h was observed in PBS at pH 7.4,  
7 indicating that the DOX-loaded micelles can preserve the core-shell architectures at  
8 physiological pH and maintain a slow diffusion with a sustained release. However, when the  
9 micelles were dispersed in an acidic environment (pH 5.0), the encapsulated DOX molecules  
10 were rapidly released on account of pH-induced quick demicellization, exhibiting much faster  
11 release rate with 49.1% contents in the first 4 h and up to 74.7% in 24 h. This pH change from  
12 extracellular environment (pH 7.4) to the endosomal compartments (pH 5.0) suggested that the  
13 DOX-loaded micelles were suitable for intracellular drug delivery. It is noted that the positive  
14 charged core of the micelles and its capacity of disrupting endosomes, due to the proton sponge  
15 effects, may further promote the application of the micelles for cytoplasmic drug delivery. It is  
16 well known that the great difference of GSH level from the circulation (10-100  $\mu$ M) to the tumor  
17 cells (1-10 mM) can trigger cleavage of the disulfide bonds. Figure 4A showed that DOX release  
18 burst from the micelles in the first 2 h (24.1%), and then sharply rose into 62.6 % after 24 h in  
19 the presence of 10 mM DTT in PBS at pH 7.4. The fast release of DOX was attributed to a rapid  
20 reductive degradation of the core by high DTT concentration. Notably, the fastest and almost  
21 completely DOX release (96.9%) was observed at pH 5.0 in the presence of 10 mM DTT. These  
22 results suggested that the micelles would significantly release their loading drugs in endosomal  
23 environments.  
24  
25  
26  
27  
28  
29  
30  
31  
32  
33  
34  
35  
36  
37  
38  
39  
40  
41  
42  
43  
44  
45  
46  
47  
48  
49  
50  
51  
52  
53  
54  
55  
56  
57  
58  
59  
60

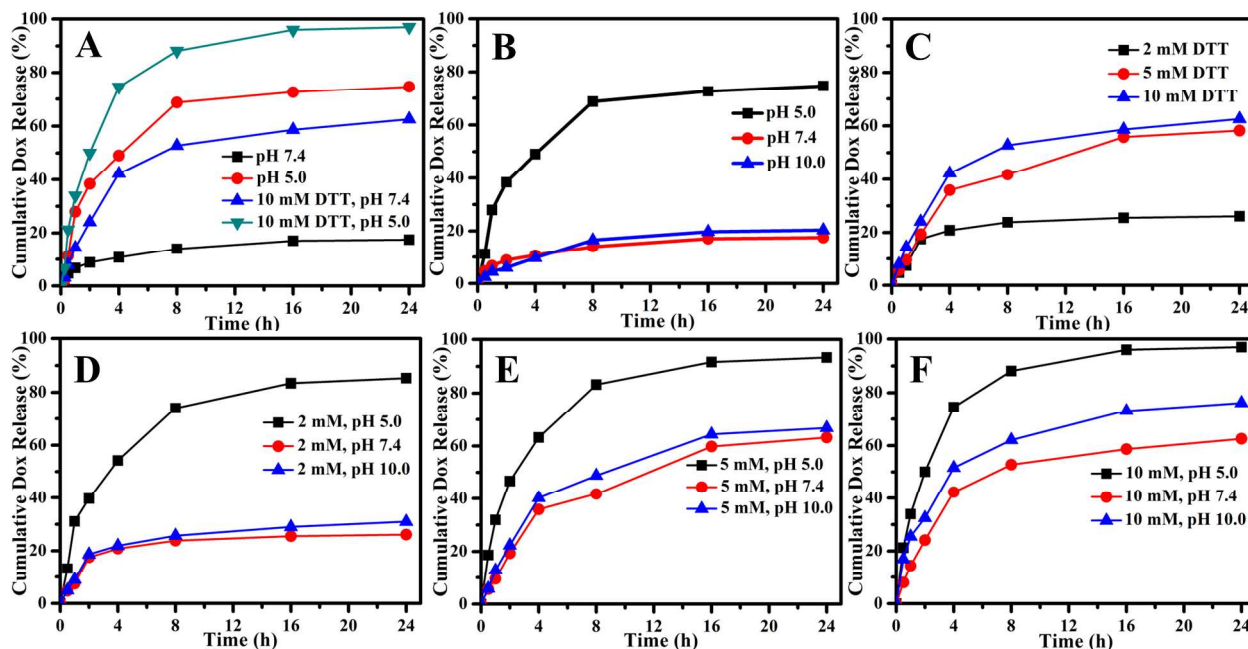
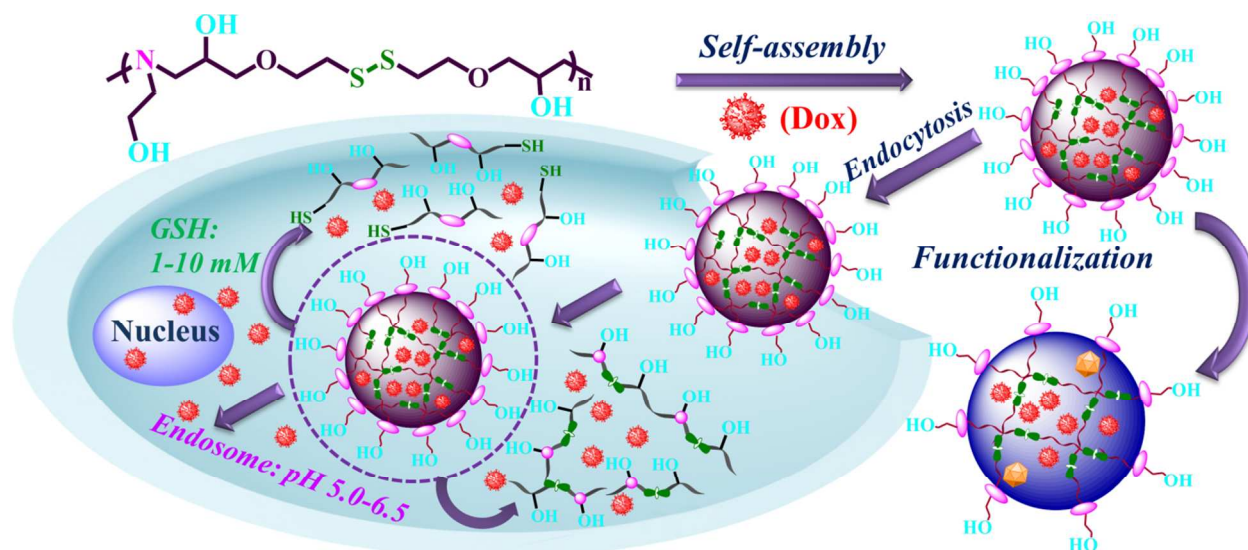


**Figure 4.** pH and/or redox-triggered release of DOX from RPHA micelles with various treatment condition at 37 °C as a function of time.

In order to further mimic the intracellular trafficking pathway and clarify the mechanism that accelerated the DOX release from the micelles, we performed the other tests including pH trend experiments: pH 5.0, 7.4 and 10.0 with and without DTT, and DTT trend experiments: 2 mM, 5 mM and 10 mM at various pH values (5.0, 7.4 and 10.0). The results disclosed that both DTT and pH worked in tandem to accelerate DOX release from the micelles. In the pH-induced degradation experiments (Figure 4B), less than 20% DOX was released from the micelles in pH 7.4 and pH 10.0 after 8 hours, but acidic environment quickly prompted DOX release (68% in pH 5.0). In the DTT-triggered degradation experiments (Figure 4C), high level of DTT concentrations can quickly disrupt the micelles and promote DOX release (42% and 53% for 5 mM and 10 mM at 8 h), while 2 mM DTT cannot effectively disintegrate micelles and only 20% DOX release was detected. After further testing with various pH and DTT concentration for 8 h

(Figure 4D-F), the DOX release can quickly increase up to 88% in the presence of pH 5.0 and 10 mM DTT, testifying that the synergistic effects of pH and DTT worked in tandem to induce demicellization and accelerate DOX release from the micelles. It was noted that DTT can improve its capacity to break the disulfide linkages in alkaline environment, so the rate of DOX release with pH 10.0 is quicker than that with pH 7.4 in the same DTT concentrations. Based on the above analysis, it is reasonable that the micelles not only possessed good stability at physiological conditions, but also had capacity to rapidly and thoroughly drug release by pH and reduction dual-stimuli in the process of intracellular trafficking.

**Scheme 3.** Activated Intracellular Drug Release from pH and GSH Dual-Sensitive Biodegradable Micelles



**Intracellular Drug Release and Antitumor Activity of DOX-Loaded RPHA Micelles.** The cellular uptake and intracellular drug release behaviours of DOX-loaded micelles (Scheme 3) were investigated using fluorescent microscope in MCF-7 cells. As displayed in Figure 5A, the DOX molecules exhibited high fluorescence intensity in the cells, indicating the rapid DOX

1  
2  
3 release from the micelles and the localization in the cells. The intracellular distribution of DOX  
4  
5 reflected that the synergistic effects of DTT-responsive degradation of disulfide linkages and pH-  
6  
7 induced quick demicellization accelerated the intracellular DOX release from the micelles. The  
8  
9 *in vitro* cytotoxicity to MCF-7 cells of the micelles was determined by CCK-8 assay. As shown  
10  
11 in Figure 5B, RPHA micelles were nontoxic to MCF-7 cells due to their low charge density and  
12  
13 quick degradation capacity in the presence of high levels of reductive agents. The cell viability  
14  
15 was more than 95% until a tested concentration of 1.0 mg/mL, demonstrating excellent  
16  
17 biocompatibility of these biodegradable micelles. However, the DOX-loaded micelles displayed  
18  
19 high efficiency of antitumor activity towards MCF-7 cells following 24 h of incubation. Figure  
20  
21 5C showed that the DOX-loaded micelles had a similar toxicity as free DOX in a low  
22  
23 concentration. In a high concentration, DOX molecules can diffuse into cells rapidly, whereas  
24  
25 the assembled micelles have to be endocytosed to enter the cells, which made free DOX  
26  
27 molecules quicker than the DOX-loaded micelles in internalization, thus presenting high  
28  
29 efficiency in cancer cell inhibition. The half-maximal inhibitory concentration ( $IC_{50}$ ) of the  
30  
31 DOX-loaded micelles was about 7.3  $\mu\text{g/mL}$  while that of free DOX was only 0.9  $\mu\text{g/mL}$ .  
32  
33 However, it should be noted that the anti-tumor activity of the micelles might be enhanced like  
34  
35 traditional carriers using targeting ligands, such as folic acid, peptide, aptamer, antibody or  
36  
37 antibody fragments, to facilitate efficient and specific cellular uptake of micelles.<sup>17</sup> The results  
38  
39 revealed that the biodegradable micelles possessed an excellent biocompatibility and the DOX-  
40  
41 loaded micelles showed a good anti-tumor capacity.  
42  
43  
44  
45  
46  
47  
48  
49  
50  
51  
52  
53  
54  
55  
56  
57  
58  
59  
60

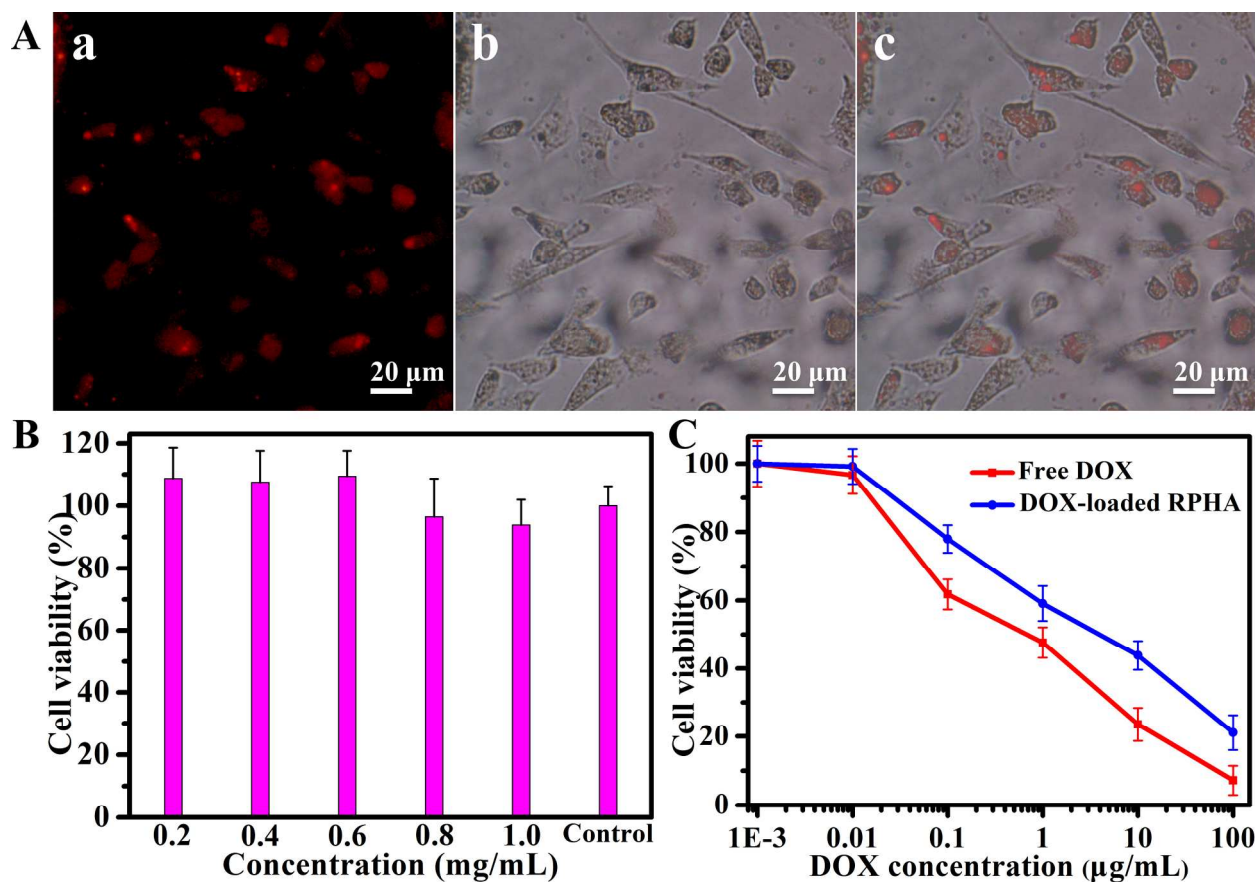


**Figure 5.** (A) Fluorescent microscope images of MCF-7 cells for cellular uptake. a: red fluorescence image; b: a bright field image; c: overlap of fluorescence and bright field images. (B) Cytotoxicity of RPHA micelles to MCF-7 cells following 24 h incubation. (C) Viabilities of MCF-7 cells following 24 h incubation with DOX-loaded RPHA micelles and free DOX as a function of DOX dosages. All the data are presented as the average  $\pm$  standard deviation.

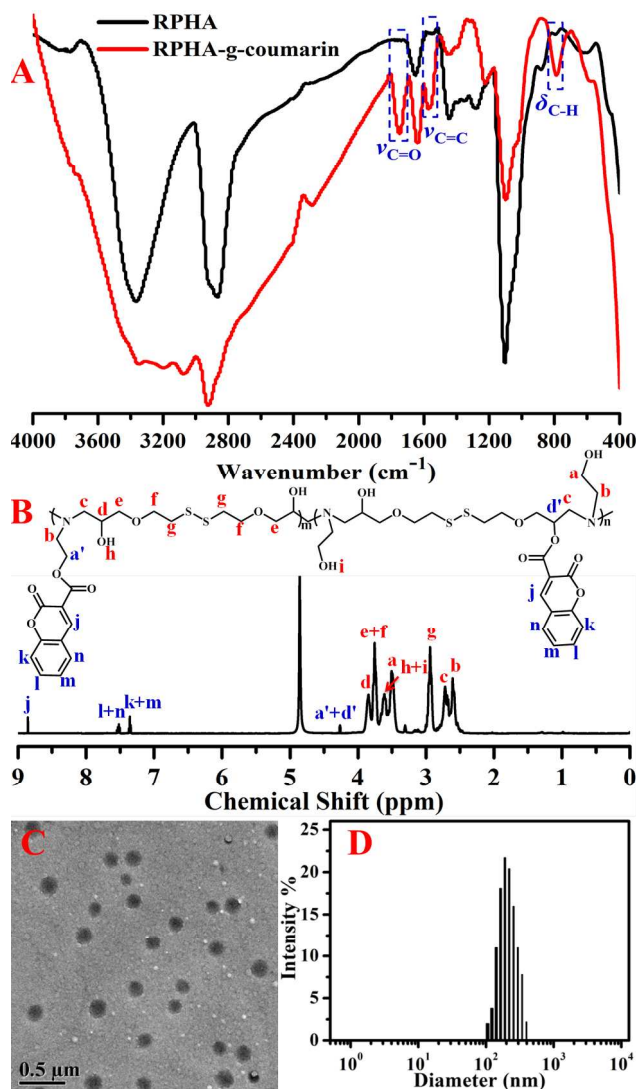


**Figure 6.** (A) IR spectra of RPHA and RPHA-g-coumarin polymers. (B) <sup>1</sup>H NMR spectrum of RPHA-g-coumarin polymer. (C) TEM image and (D) DLS plot of RPHA-g-coumarin micelles.

Coumarin and its derivatives type dyestuff, possessing high fluorescent efficiency, are used in the fields of biology, medicine, perfumes and cosmetics, cigarettes, alcoholic beverages, laser dyes and polymer science.<sup>18,19</sup> On account of abundant hydroxyl groups that can be facilely modified, a RPHA-g-coumarin polymer was obtained by acylation reaction with a small amount of coumarins anchoring on the side chain shown in Scheme 1. IR spectra gave an evidence to

1  
2  
3 demonstrate the effective attachment on RPHA polymer with coumarins in Figure 6A.  $^1\text{H}$  NMR  
4 spectrum showed the typical signals of coumarin groups (j-n) at 7.35, 7.52 and 8.86 ppm as well  
5  
6 as the new peaks of a' and d' at 4.25-4.28 ppm for the RPHA-g-coumarin polymer in Figure 6B.  
7  
8 The integration ratio ( $I_j/I_g$ ) was close to 1:60, indicating the grafting rate of the coumarin was  
9  
10 about 3.3%. Figure 6C disclosed the uniform sphere micelles with the size of 145 nm assembled  
11  
12 by the RPHA-g-coumarin polymer, but the average diameter (195 nm) with a PDI of 0.379 from  
13  
14 the DLS result in Figure 6D was a little bigger than that of the RPHA micelles (185 nm, Figure  
15  
16 2D). The increase of the micellar size may be attributed to the faint increase of hydrophobicity.  
17  
18 Controlling low grafting rates of coumarins not only aimed to keep the RPHA-g-coumarin  
19  
20 micelles stable in an aqueous solution, but also ensure the optimal size of the micelles for  
21  
22 intracellular drug delivery. Although the percentage of coumarin molecules was low, the RPHA-  
23  
24 g-coumarin polymer presented strong UV absorption and fluorescence intensity as shown in  
25  
26 Figure 7A and 7B. Confocal laser scanning microscopy (CLSM) in Figure 7C and 7D provided  
27  
28 intuitive structural insights to better observe the RPHA-g-coumarin polymer and RPHA-g-  
29  
30 coumarin micelles with high intense fluorescence. Importantly, compared to the encapsulated  
31  
32 dyes in the micelles, covalent conjugated coumarins are stable with a period of time in aqueous  
33  
34 solutions, which would be useful for application of fluorescence labelling. The further study of  
35  
36 coumarin-based biodegradable micelles with multiple responses is an intriguing ongoing work in  
37  
38 our laboratory and will be discussed in future publications.  
39  
40  
41  
42  
43  
44  
45  
46  
47  
48

49 The functional modification with excessive hydroxyl groups by acylation reaction is a general  
50  
51 strategy to produce smart multi-responsive materials. Currently we have also synthesized a  
52  
53 paclitaxel-conjugated RPHA polymer, and obtained dual-drugs loaded biodegradable micelles by  
54  
55  
56  
57  
58  
59  
60

manipulating self-assembly condition to encapsulate DOX drugs, which presented the excellent antitumor activity in targeted cells with pH and reduction dual-responsiveness.

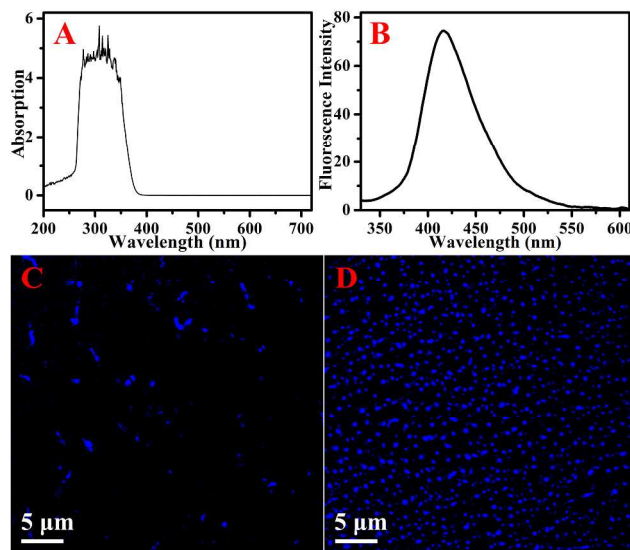


**Figure 7.** (A) Absorption spectrum, (B) Emission spectrum ( $\lambda_{\text{ex}} = 314 \text{ nm}$ ) and (C) CLSM image of RPHA-g-coumarin polymer in methanol. (D) CLSM image of RPHA-g-coumarin micelles.

## CONCLUSION

In summary, we synthesized a kind of main-chain cationic polymer (RPHA) with a large number of hydroxyl groups, disulfide linkages and tertiary amines. This polymer assembled into uniform sphere micelles in aqueous solutions with pH and reduction dual-responsive biodegradation. The DOX-loaded micelles can preserve the core-shell architectures in the normal physiological conditions, and rapidly release the drug in the presence of high level of reductive agent and/or acidic environment, which mimics the pH and reduction conditions in the endosomes. Cytotoxicity assay of the DOX-loaded micelles indicated a fast internalization and a high cellular proliferation inhibition to MCF-7 cells. After further functionalization with excessive hydroxyl groups by acylation reaction, the RPHA polymer was facilely modified into the multifunctional

1  
2  
3 nanocarriers, paving a new pathway for acquiring intelligent biomaterials in the field of  
4  
5 fluorescent probe, bioimaging, drug delivery and biomedicine.  
6  
7

## 8 9 AUTHOR INFORMATION

### 10 11 **Corresponding Author**

12  
13  
14 \*E-mail: dcwu@iccas.ac.cn; wangxing@iccas.ac.cn  
15  
16

### 17 18 **Author Contributions**

19  
20 <sup>1</sup>Dawei Li and Yazhong Bu contributed equally to this work.  
21  
22

### 23 24 **Notes**

25  
26  
27 The authors declare no competing financial interests.  
28  
29

### 30 31 **ACKNOWLEDGMENT**

32 We gratefully acknowledge MOST (2014CB932200 and 2014BAI11B04), ‘Young Thousand  
33  
34 Talents Program’ and NSFC (21504096, 21174147 and 21474115) for financial support.  
35  
36

### 37 38 **REFERENCES**

- 39  
40 (1) (a) Gao, X.; Wang, S. M.; Wang, B. L.; Deng, S. Y.; Liu, X. X.; Zhang, X. N.; Luo, L. L.;  
41 Fan, R. R.; Xiang, M. L.; You, C.; Wei, Y. Q.; Qian, Z. Y.; Guo, G. *Biomaterials* **2015**, *53*,  
42 646–658. (b) Chen, W.; Meng, F. H.; Cheng, R.; Deng, C.; Feijen, J.; Zhong, Z. Y. *J. Control.*  
43 *Release* **2015**, *210*, 125–133. (c) Li, Y. L.; Zhu, L.; Liu, Z. Z.; Cheng, R.; Meng, F. H.; Cui, J. H.;  
44 Ji, S. J.; Zhong, Z. Y. *Angew. Chem., Int. Ed.* **2009**, *48*, 9914–9918.  
45  
46 (2) (a) Cui, H. G.; Chen, Z. Y.; Zhong, S.; Wooley, K. L.; Pochan, D. J. *Science* **2007**, *317*,  
47 647–650. (b) Nicolas, J.; Mura, S.; Brambilla, D.; Mackiewicz, N.; Couvreur, P. *Chem. Soc. Rev.*  
48 **2013**, *42*, 1147–1235. (c) Ebrahim, A.; Amalina, B.; Oh, P.; Yang, C.; Tan, J. P. K.; Rao, N.;  
49 Hedrick, J. L.; Yang, Y. Y.; Ge, R. W. *Small* **2014**, *10*, 4281–4286. (d) Xu, P. S.; Van Kirk, E.  
50 A.; Zhan, Y. H.; Murdoch, W. J.; Radosz, M.; Shen, Y. Q. *Angew. Chem., Int. Ed.* **2007**, *46*,  
51 4999–5002.  
52  
53 (3) (a) Huang, P. S.; Wang, W. W.; Zhou, J. H.; Zhao, F. L.; Zhang, Y. M.; Liu, J. J.; Liu, J.  
54 F.; Dong, A. J.; Kong, D. L.; Zhang, J. H. *ACS Appl. Mater. Interfaces* **2015**, *7*, 6340–6350. (b)  
55 Chen, Y. S.; Wu, Q. J.; Song, L. J.; He, T.; Li, Y. C.; Li, L.; Su, W. J.; Liu, L.; Qian, Z. Y.;  
56 Gong, C. Y. *ACS Appl. Mater. Interfaces* **2015**, *7*, 534–542. (c) Zhang, Q.; Vakili, M. R.; Li, X.  
57  
58  
59  
60

1  
2  
3 F.; Lavasanifar, A.; Le, X. C. *Biomaterials* **2014**, *35*, 7088–7100. (d) Lee, M.; Jeong, J.; Kim, D.  
4 *Biomacromolecules* **2015**, *16*, 136–144. (e) Louage, B.; Zhang, Q. L.; Vanparijs, N.; Voorhaar,  
5 L.; Vande Castele, S.; Shi, Y.; Hennink, W. E.; Van Bocxlaer, J.; Hoogenboom, R.; De Geest,  
6 B. G. *Biomacromolecules* **2015**, *16*, 336–350.

7  
8 (4) (a) Wang, J. R.; Sun, X. R.; Mao, W. W.; Sun, W. L.; Tang, J. B.; Sui, M. H.; Shen, Y. Q.;  
9 Gu, Z. W. *Adv. Mater.* **2013**, *25*, 3670–3676. (b) Zhou, Z. X.; Ma, X. P.; Murphy, C. J.; Jin, E.  
10 L.; Sun, Q. H.; Shen, Y. Q.; Van Kirk, E. A.; Murdoch, W. J. *Angew. Chem., Int. Ed.* **2014**, *53*,  
11 10949–10955. (c) Sun, Q. H.; Sun, X. R.; Ma, X. P.; Zhou, Z. X.; Jin, E. L.; Zhang, B.; Shen, Y.  
12 Q.; Van Kirk, E. A.; Murdoch, W. J.; Lott, J. R.; Lodge, T. P.; Radosz, M.; Zhao, Y. L. *Adv.*  
13 *Mater.* **2014**, *45*, 7615–7621. (d) Zhou, Z. X.; Shen, Y. Q.; Tang, J. B.; Fan, M. H.; Van Kirk, E.  
14 A.; Murdoch, W. J.; Radosz, M. *Adv. Funct. Mater.* **2009**, *19*, 3580–3589.

15  
16 (5) (a) Rosler, A.; Vandermeulen, G. W. M.; Klok, H. A. *Adv. Drug Delivery Rev.* **2012**, *64*,  
17 270–279. (b) Owen, S. C.; Chan, D. P. Y.; Shoichet, M. S. *Nano Today* **2012**, *7*, 53–65. (c)  
18 Gupta, R.; Shea, J.; Scafe, C.; Shurlygina, A.; Rapoport, N. *J. Control. Release* **2015**, *212*, 70–77.

19  
20 (6) (a) Chen, W. C.; Yuan, Y. Y.; Cheng, D.; Chen, J. F.; Wang, L.; Shuai, X. T. *Small* **2014**,  
21 *10*, 2678–2687. (b) Chen, C. Y.; Kim, T. H.; Wu, W. C.; Huang, C. M.; Wei, H.; Mount, C. W.;  
22 Tian, Y. Q.; Jang, S. H.; Pun, S. H.; Jen, A. K. Y. *Biomaterials* **2013**, *34*, 4501–4509. (c) Peng,  
23 L.; Feng, A. C.; Zhang, H. J.; Wang, H.; Jian, C. M.; Liu, B. W.; Gao, W. P.; Yuan, J. Y. *Polym.*  
24 *Chem.* **2014**, *5*, 1751–1759. (d) Kelley, E. G.; Albert, J. N. L.; Sullivan, M. O.; Epps, T. H.  
25 *Chem. Soc. Rev.* **2013**, *42*, 7057–7520. (e) Guo, X.; Shi, C. L.; Yang, G.; Wang, J.; Cai, Z. H.;  
26 Zhou, S. B. *Chem. Mater.* **2014**, *26*, 4405–4418. (f) Guo, X.; Shi, C. L.; Wang, J.; Di, S. B.;  
27 Zhou, S. B. *Biomaterials* **2013**, *34*, 4544–4554.

28  
29 (7) (a) Cain, C. C.; Sipe, D. M.; Murphy, R. F. *Proc. Natl. Acad. Sci.* **1989**, *86*, 544–548. (b)  
30 Binauld, S.; Stenzel, M. H. *Chem. Commun.* **2013**, *49*, 2082–2102. (c) Meng, F.; Zhong, Y.;  
31 Cheng, R.; Deng, C.; Zhong, Z. *Nanomedicine* **2014**, *9*, 487–499. (d) Yang, Y. Y.; Hu, H.; Wang,  
32 X.; Yang, F.; Shen, H.; Xu, F. J.; Wu, D. C. *ACS Appl. Mater. Interfaces* **2015**, *7*, 12238–12248.  
33 (e) Huang, D.; Li, D. W.; Wang, T. T.; Shen, H.; Zhao, P.; Liu, B. X.; You, Y. Z.; Ma, Y. Z.;  
34 Yang, F.; Wu, D. C. *Biomaterials* **2015**, *52*, 417–426.

35  
36 (8) (a) Kim, D. H.; Seo, Y. K.; Thambi, T.; Moon, G. L.; Son, J. P.; Li, G.; Park, J. H.; Lee,  
37 J. H.; Kim, H. H.; Lee, D. S.; Bang, O. Y. *Biomaterials* **2015**, *61*, 115–125. (b) Qiao, Z. Y.;  
38 Qiao, S. L.; Fan, G.; Fan, Y. S.; Chen, Y.; Wang, H. *Polym. Chem.* **2014**, *5*, 844–853. (c) Li, Y.  
39 P.; Xiao, K.; Zhu, W.; Deng, W.; Lam, K. S. *Adv. Drug Delivery Rev.* **2014**, *66*, 58–73.

40  
41 (9) (a) Chiang, Y. T.; Yen, Y. W.; Lo, C. L. *Biomaterials* **2015**, *61*, 150–161. (b) Hu, Y. W.;  
42 Du, Y. Z.; Liu, N.; Liu, X.; Meng, T. T.; Cheng, B. L.; He, J. B.; You, J.; Yuan, H.; Hu, F. Q. *J.*  
43 *Control. Release* **2015**, *206*, 91–100. (c) Liu, R.; Zhao, X.; Wu, T.; Feng, P. Y.; Amir, J. *J. Am.*  
44 *Chem. Soc.* **2008**, *130*, 14418–14419. (d) Shi, C. L.; Guo, X.; Qu, Q. Q.; Tang, Z. M.; Wang, Y.;  
45 Zhou, S. B. *Biomaterials* **2014**, *35*, 8711–8722. (e) Wang, J.; Yang, G.; Guo, X.; Tang, Z. M.;  
46 Zhong, Z. D.; Zhou, S. B. *Biomaterials*, **2014**, *35*, 3080–3090. (f) Yang, Y. Y.; Wang, X.; Hu,  
47 Y.; Hu, H.; Wu, D. C.; Xu, F. J. *ACS Appl. Mater. Interfaces* **2014**, *6*, 1044–1052. (g) Zhang, J.;  
48 Yang, F.; Shen, H.; Wu, D. C. *ACS Macro Lett.* **2012**, *1*, 1295–1299.

49  
50 (10) (a) Hwang, C.; Sinskey, A. J.; Lodish, H. F. *Science* **1992**, *257*, 1496–1502. (b) Roy, D.;  
51 Cambre, J. N.; Sumerlin, B. S. *Prog. Polym. Sci.* **2010**, *35*, 278–301. (c) Wang, X.; Li, D.; Yang,  
52 F.; Shen, H.; Li, Z. B.; Wu, D. C. *Polym. Chem.* **2013**, *4*, 4596–4600. (d) Huo, M.; Yuan, J.; Tao,  
53 L.; Wei, Y. *Polym. Chem.* **2014**, *5*, 1519–1528. (e) Yang, Q. L.; Tan, L. J.; He, C. Y.; Liu, B. Y.;  
54 Xu, Y. H.; Zhu, Z. G.; Shao, Z. F.; Gong, B.; Shen, Y. M. *Acta Biomater.* **2015**, *17*, 193–200. (f)  
55 Chen, W.; Zou, Y.; Junna, J.; Meng, F. H.; Cheng, R.; Deng, C.; Feijen, J.; Zhong, Z. Y.  
56  
57  
58  
59  
60

1  
2  
3  
4  
5  
6  
7  
8  
9  
10  
11  
12  
13  
14  
15  
16  
17  
18  
19  
20  
21  
22  
23  
24  
25  
26  
27  
28  
29  
30  
31  
32  
33  
34  
35  
36  
37  
38  
39  
40  
41  
42  
43  
44  
45  
46  
47  
48  
49  
50  
51  
52  
53  
54  
55  
56  
57  
58  
59  
60

*Macromolecules* **2013**, *46*, 699–707. (g) Wu, D. C.; Loh, X. J.; Wu, Y. L.; Lay, C. L.; Liu, Y. J. *Am. Chem. Soc.* **2010**, *132*, 15140–15143.

(11) (a) Hu, J. M.; Wang, X.; Qian, Y. F.; Yu, Y. Q.; Jiang, Y. Y.; Zhang, G. Y.; Liu, S. Y.; *Macromolecules* **2015**, *48*, 5959–5968. (b) Ding, M. M.; Zeng, X.; He, X. L.; Li, J. H.; Tan, H.; Fu, Q. *Biomacromolecules* **2014**, *15*, 2896–2906. (c) Liu, J.; Huang, Y. R.; Kumar, A.; Tan, A.; Jin, S. B.; Mozhi, A.; Liang, X. J. *Biotechnol. Adv.* **2014**, *32*, 693–710. (d) Hu, J.; Miura, S.; Na, K.; Bae, Y. H. *J. Control. Release* **2013**, *172*, 69–76. (e) Zhao, Y.; Zhou, Y. X.; Wang, D. S.; Gao, Y. J.; Li, J. W.; Ma, S. J.; Zhao, L.; Zhang, C.; Liu, Y.; Li, X. R. *Acta Biomater.* **2015**, *17*, 182–192.

(12) (a) Tian, H. Y.; Deng, C.; Lin, H.; Sun, J. R.; Deng, M. X.; Chen, X. S.; Jing, X. B. *Biomaterials* **2005**, *26*, 4209–4217. (b) Li, L.; Sun, W.; Zhong, J. J.; Yang, Q. Q.; Zhu, X.; Zhou, Z.; Zhang, Z. R.; Huang, Y. *Adv. Funct. Mater.* **2015**, *25*, 4101–4113. (c) Cabral, H.; Kataoka K., *J. Control. Release* **2014**, *190*, 465–476. (d) Yim, H.; Park, W.; Kim, D.; Fahmy, T. M.; Na, K. *Biomaterials* **2014**, *35*, 9912–9919. (e) Song, X. J.; Zhang, R.; Liang, C.; Chen, Q.; Gong, H.; Liu, Z. *Biomaterials* **2015**, *57*, 84–92.

(13) (a) Park, T. G.; Jeong, J. H.; Kim, S. W. *Adv. Drug Delivery Rev.* **2006**, *58*, 467–486. (b) Loh, X. J.; Wu, Y. L. *Chem. Commun.* **2015**, *51*, 10815–10818. (c) Li, Y.; Wang, Y. G.; Huang, G.; Ma, X. P.; Zhou, K. J.; Gao, J. M. *Angew. Chem., Int. Ed.* **2014**, *53*, 8074–8078. (d) Kozielski, K. L.; Tzeng, S. Y.; De Mendoza, B. A. H.; Green, J. J. *ACS Nano* **2014**, *8*, 3232–3241. (e) Nuhn, L.; Gietzen, S.; Mohr, K.; Fischer, K.; Toh, K.; Miyata, K.; Matsumoto, Y.; Kataoka, K.; Schmidt, M.; Zentel, R. *Biomacromolecules* **2014**, *15*, 1526–1533. (f) Li, Y.; Liu, R. Y.; Yang, J.; Ma, G. H.; Zhang, Z. Z.; Zhang, X. *Biomaterials* **2014**, *35*, 9731–9745.

(14) (a) Saha, A.; De, S.; Stuparu, M. C.; Khan, A. *J. Am. Chem. Soc.* **2012**, *134*, 17291–17197. (b) Cano, M.; Cueva-Mendez, G. de la *Chem. Commun.* **2015**, *51*, 3620–3622. (c) Tanaka, Y.; Stanford, J. L.; Stepto, R. *Macromolecules* **2012**, *45*, 7186–7196. (d) Pratama, P. A.; Peterson, A. M.; Palmese, G. R. *Polym. Chem.* **2013**, *4*, 5000–5006.

(15) (a) Chen, J.; Qiu, X. Z.; Ouyang, J.; Kong, J.; Zhong, W.; Xing, M. M. *Q. Biomacromolecules* **2011**, *12*, 3601–3611. (b) Zhang, C. N.; Jin, R.; Zhao, P.; Lin, C. *Acta Biomater.* **2015**, *22*, 120–130.

(16) (a) Schmalenberg, K. E.; Frauchiger, L.; Nikkhouy-Albers, L.; Uhrich, K. E. *Biomacromolecules* **2001**, *2*, 851–855. (b) Liu, J. Y.; Pang, Y.; Huang, W.; Huang, X. H.; Meng, L. L.; Zhu, X. Y.; Zhou, Y. F.; Yan, D. Y. *Biomacromolecules* **2011**, *12*, 1567–1577.

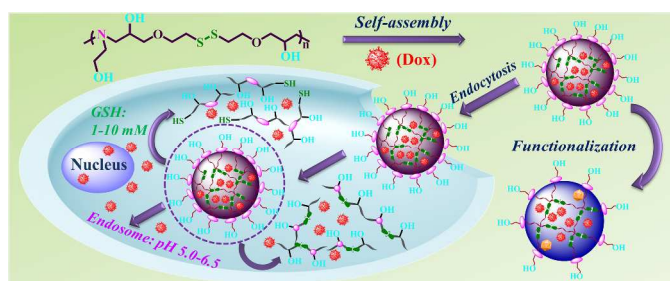
(17) (a) Qian, X. M.; Peng, X. H.; Ansari, D. O.; Yin-Goen, Q.; Chen, G. Z.; Shin, D. M.; Yang, L.; Young, A. N.; Wang, M. D.; Nie, S. M. *Nat. biotechnol.* **2008**, *26*, 83–90. (b) Shuker, S. B.; Hajduk, P. J.; Meadows, R. P.; Fesik, S. W. *Science* **1996**, *274*, 1531–1534. (c) Ricote, M.; Li, A. C.; Willson, T. M.; Kelly, C. J.; Glass, C. K. *Nature* **1998**, *391*, 79–82. (d) Gao, X. H.; Cui, Y. Y.; Levenson, R. M.; Chung, L. W. K.; Nie, S. M. *Nat. biotechnol.* **2004**, *22*, 969–976. (e) Shen, Q.; Jin, E. L.; Zhang, B.; Murphy, C. J.; Sui, M. H.; Zhao, J.; Wang, J. Q.; Tang, J. B.; Fan, M. H.; Van Kirk, E. A.; Murdoch, W. J. *J. Am. Chem. Soc.* **2010**, *132*, 4259–4265.

(18) (a) Trenor, S. R.; Shultz, A. R.; Love, B. J.; Long, T. E. *Chem. Rev.* **2004**, *104*, 3059–3078. (b) Win, K. Y.; Feng, S. S. *Biomaterials* **2005**, *26*, 2713–2722. (c) Wu, M. Y.; Li, K.; Liu, Y. H.; Yu, K. K.; Xie, Y. M.; Zhou, X. D.; Yu, X. Q. *Biomaterials* **2015**, *53*, 669–678. (d) Tran, T. M.; Alan, Y.; Glass, T. E. *Chem. Commun.* **2015**, *51*, 7915–7918. (e) Draper, E. R.; McDonald, T. O.; Adams, D. J. *Chem. Commun.* **2015**, *51*, 12827–12830. (f) Tian, H. Y.; Qian, J. H.; Sun, Q.; Jiang, C. J.; Zhang, R. S.; Zhang, W. B. *Analyst* **2014**, *139*, 3373–3377.

- 1  
2  
3 (19) (a) Rosenbaum, I.; Harnoy, A. J.; Tirosh, E.; Buzhor, M.; Segal, M.; Frid, L.;  
4 Shaharabani, R.; Avinery, R.; Beck, R.; Amir, R. J. *J. Am. Chem. Soc.* **2015**, *137*, 2276–2284.  
5 (b) Okazawa, Y.; Kondo, K.; Akita, M.; Yoshizawa, M. *J. Am. Chem. Soc.* **2015**, *137*, 98–101.  
6 (c) Chen, S.; Jiang, F. J.; Cao, Z. Q.; Wang, G. J.; Dang, Z. M. *Chem. Commun.* **2015**, *51*,  
7 12633–12636. (d) Albright, T. R.; Winter, A. H. *J. Am. Chem. Soc.* **2015**, *137*, 3402–3410.  
8  
9  
10  
11  
12  
13  
14  
15  
16  
17  
18  
19  
20  
21  
22  
23  
24  
25  
26  
27  
28  
29  
30  
31  
32  
33  
34  
35  
36  
37  
38  
39  
40  
41  
42  
43  
44  
45  
46  
47  
48  
49  
50  
51  
52  
53  
54  
55  
56  
57  
58  
59  
60

## Table of Contents

### Title: Facile Construction of pH- and Redox-Responsive Micelles from a Biodegradable Poly( $\beta$ -hydroxyl amine) for Drug Delivery



The biodegradable micelles, assembled by a reductive poly( $\beta$ -hydroxyl amine), possess pH and redox dual-responsiveness for targeting drug delivery.

---